Academic Sciences International Journal of Pharmacy and Pharmaceutical Sciences

ISSN- 0975-1491 Vol 6, Issue 2, 2014

Research Article

MICROTUBULE DISRUPTING N-PHENYL-N'-(2-CHLOROETHYL) UREAS DISPLAY ANTICANCER ACTIVITY ON CELL ADHESION, P-GLYCOPROTEIN AND BCL-2-MEDIATED DRUG RESISTANCE

JESSICA S. FORTIN[1], MARIE-FRANCE CÔTÉ[2], RÉNA G. DESCHESNES[2], ALEXANDRE PATENAUDE[•], JACQUES LACROIX[2], MARIE-ODILE BENOIT-BIANCAMANO[1] AND RENÉ C.-GAUDREAULT[2]

[1]Faculté de médecine vétérinaire, Département de pathologie et microbiologie, Université de Montréal, 3200 Sicotte, St-Hyacinthe, QC, J2S 2M2. [2]Centre de recherche, Unité de Biotechnologie et de Bioingénierie, C.H.U.Q., Hôpital Saint-François d'Assise, 10 rue de l'Espinay, Québec, Québec, Canada, G1L 3L5. [2]Faculté de médecine, Université Laval, Sainte-Foy, Québec, Canada, G1V 0A6. Email: rene.c-gaudreault@crsfa.ulaval.ca (RCG),Jessica.fortin.2@umontreal.ca (JF)

Received: 03 Jan 2014, Revised and Accepted: 20 Feb 2014

ABSTRACT

Objective: Our research program has focused on the development of promising, soft alkylating *N*-phenyl-*N'*-(2-chloroethyl)urea (CEU) compounds which acylate the glutamic acid-198 of β-tubulin, near the binding site of colchicum alkaloids. CEUs inhibit the motility of cancerous cells *in vitro* and, interestingly, exhibit antiangiogenic and anticancer activity *in vivo*. Mitotic arrest induced by microtubule-interfering agents such as CEUs remains the major mechanism of their anticancer activity, leading to apoptosis. However, we recently demonstrated that microtubule disruption by CEUs and other common antimicrotubule agents greatly alters the integrity and organization of microtubule-associated structures, the focal adhesion contact, thereby initiating anoikis, an apoptosis-like cell death mechanism caused by the loss of cell contact with the extracellular matrix.

Methods: To ascertain the activated signaling pathway profile of CEUs, flow cytometry, Western blot, immunohistochemistry and transfection experiments were performed. Wound-healing and chick embryo assays were carried out to evaluate the antiangiogenic potency of CEUs.

Results: CEU-induced apoptosis involved early cell cycle arrest in G_2/M and increased level of CDK1/cycline B proteins. These signaling events were followed by the specific activation of the intrinsic apoptosis pathway, involving loss of mitochondrial membrane potential ($\Delta\psi_m$) and ROS production, cytochrome c release from mitochondria, caspase activation, AIF nuclear translocation, PARP cleavage and nuclear fragmentation. CEUs maintained their efficacy on cells plated on pro-survival extracellular matrices or exhibiting overexpression of P-glycoprotein or the anti-apoptotic protein Bcl-2.

Conclusion: Our results suggest that CEUs represent a promising new class of antimicrotubule, antiangiogenic and pro-anoikis agents.

Keywords: Aryl chloroethylureas; Mitotic agents; Resistance; Mitochondria; Anoikis.

INTRODUCTION

N-phenyl-*N'*-(2-chloroethyl) ureas (CEUs) are low-molecular weight compounds that monoalkylate proteins, exhibit antiproliferative activity on cancer cells and deeply affect microtubule dynamics [1-3]. CEUs acylate the glutamic acid-198 residue of the mouse β-tubulin isoform 5 [2]. The glutamate 198 in β-tubulin was shown to be a critical determinant for microtubule stability [4]. Competitive assays demonstrated that CEU-022 (4-*tert*-butyl-[3-(2-chloroethyl)ureido]phenyl) and several CEU drugs acylate human β-tubulin in a pocket closely adjacent to the colchicine binding site, thereby leading to microtubule depolymerization, actin cytoskeleton dissolution and, ultimately, cell death [1, 3, 5]. As opposed to DNA alkylating agents, CEU compounds have been shown as non mutagenic and unreactive towards most cellular nucleophiles, such as gluthatione and DNA. More recently, we have described that CEU-022 and CEU-098 (4-iodo-[3-(2-chloroethyl)ureido]phenyl) strongly inhibit the migration of endothelial and tumor cells and exhibit antiangiogenic properties, which were confirmed *in vivo* using the Matrigel Plug assay in mice and the chick chorioallantoic membrane assay (CAM) [1]. In addition, the antiproliferative activity of CEU-022, CEU-098 and, a new prototype, CEU-236 (N-(2-chloroethyl)-N'-[3-(hydroxypentanyl) phenyl]urea), was effective in hypoxia-resistant cells [3].

The major and common action of microtubule-interfering agents is the inhibition of the spindle microtubule dynamics, consequently leading to cell cycle blockage at the transition from prometaphase/metaphase to anaphase [6]. All microtubule-targeting agents, such as *vinca* alkaloids, taxanes and epothilones, are cytostatic, arresting cells in mitosis, and are not intrinsically able to cause cytotoxicity [7]. Persistent and sustained mitotic arrest, which is poorly tolerated by cells, leads to the disruption of cell division and [6, 8, 9] the accumulation of several signals until reaching a certain threshold for the onset of apoptosis [10]. Following antimicrotubule treatment, sustained inactivation of the anti-apoptotic protein Bcl-2 through phosphorylation induced by the stress-activated MAP kinase ASK1/JNK occurs in cells blocked at the G_2/M transition. Interestingly, phosphorylation of Bcl-2 and activation of the ASK1/JNK pathway are two signaling events normally occurring at the G_2/M phase of the cell cycle. Phosphorylation of Bcl-2 and ASK-1 transiently increase cell sensitivity to apoptosis, acting as a mechanism to limit the consequences of defects in the spindle structure or aberrant chromosomic division [10]. By inducing a permanent mitotic arrest, microtubule inhibitors therefore induce a permanent activation of these apoptotic signals normally occurring transiently during mitosis. The stress-activated MAP kinase JNK also phosphorylates the BH3-only protein Bim to potentiate its pro-apoptotic activity [11] and to promote the accumulation of active Bax in the mitochondria [12]. This phosphorylation allows the release of Bim from the microtubule-associated dynein motor complex where it is normally sequestered and induces its translocation to mitochondria. Thus, Bim binds Bcl-2 and Bcl-x_L and promotes apoptosis through neutralization of their anti-apoptotic activity or through activation of Bax [13]. The heterodimerization of Bax with Bcl-2 or Bcl-x_L is essential to trigger the permeabilization of the outer mitochondrial membrane [12, 14] and to mediate the release of pro-apoptotic proteins such as cytochrome c, Apaf-1, caspase-9, AIF, Smac/DIABLO and HtrA2/Omi to the cytosol [9, 12]. Cytochrome c complexes with Apaf-1 and caspase-9, known as the post-mitochondrial apoptosome, and amplifies the proper activation of effector caspases-3, -7 and -6 [14]. These proteases cleave specific sets of cellular and nuclear substrates, such as FAK and Akt [15], resulting in the biochemical and morphological changes associated with the apoptotic phenotype [9].

We recently found that CEU derivatives induced focal adhesion disorganization, thereby leading to anoikis [5]. Anoikis is a rapid apoptotic response to an altered cellular environment that is

initiated early after inhibition of integrin signaling. The molecular mechanisms of anoikis differ among cell types and involve diverse apoptotic pathways, such as the activation of the JNK pathway and the Fas signaling complex. Interestingly, simultaneous pharmacological disruption of actin microfilaments and microtubules have led to more pronounced cell rounding and enhanced levels of apoptosis, approaching those observed during anoikis in fully detached cells [16]. During cell rounding, the protein kinase Akt/PKB becomes dephosphorylated and Bcl-2 expression decreases. The disruption of structural elements or change in cell shape that alters microtubules and cytoskeletal structures are sufficient by themselves to initiate anoikis [16]. Accordingly, by serving as sensors for microtubules and actin cytoskeleton integrity, the pro-apoptotic BH3-only proteins Bim and Bmf were associated with anoikis [17]. While Bim is sequestered to the microtubule-associated dynein motor complex, Bmf is sequestered to actin-associated myosin V motor complex. Loss of cell attachment has been shown to unleash Bim and Bmf, allowing them to translocate and neutralize prosurvival Bcl-2 proteins [17] or induce Bax activation, leading to the activation of the intrinsic apoptosis pathway [18]. Evidence supports the assumption that adhesion-dependent changes in microtubules and cytoskeletal structures are hallmarks for the initiation of anoikis/apoptosis signal transduction cascade [16]. In the present study, we describe sustained mitotic arrest induced by CEUs such as CEU-022, -098 and -236, leading to cell death triggered by loss of focal adhesion (anoikis) and apoptosis. We demonstrate a dose-dependent effect on G_2/M cells arrest, tumor proliferation, and cell migration mediated by CEUs. We finally show that extra-cellular matrix (ECM), P-glycoprotein over expression and Bcl-2 over expression had no protective effect on tumor cell death induced by CEUs.

MATERIALS AND METHODS

Reagents and Chemicals: N-(2-chloroethyl)-N'-[4-(1,1-dimethylethyl) phenyl]urea (**CEU-022**), N-(2-chloroethyl)-N'-(4-iodophenyl)urea (**CEU-098**), N-(2-chloroethyl)-N'-[3-(hydroxypentanyl) phenyl]urea (**CEU-236**) and N-[4-(1,1-dimethylethyl)-N'-ethylurea (**CEU-091**) were prepared as published previously. All drugs were dissolved in DMSO to make stock solutions of 40 mM. DMSO final concentration in the culture medium was maintained under 0.2 % (v/v) for each assay. Vinblastine sulfate and colchicine were purchased from Sigma (St-Louis, MA) and *N*-benzyloxycarbonyl-Val-Ala-Asp-fluoromethylketone (zVAD.fmk) from Bachem Bioscience inc. (King of Prussia, PA). Chemicals for electrophoresis were purchased from Bio-rad (Hercules, CA) and Sigma (St-Louis, MA).

Cell lines and Culture: Human skin melanoma M21 cells were kindly provided by Dr. David A. Cheresh (The Scripps Research Institute, San Diego, CA). HT1080 (human fibrosarcoma), HT-29 (human colon carcinoma) and MDA-MB-231 (human breast carcinoma) cells were purchased from American Type Culture Collection (ATCC) and cultured in DMEM supplemented with 5% fetal bovine serum. CEM and CEM-VLB cells were kindly provided by Dr. William T. Beck and were cultured in RPMI supplemented with 10% fetal calf serum.

Antibodies: Anti-cyclin A, B, and D3, as well as CDK1, CDK2 and CDK4, and PARP antibodies were obtained from BD Transduction Laboratories (Mississauga, ON). Mouse antibodies against cyclin E (HE-12) was purchased from Santa Cruz Biotechnology (Santa Cruz, CA), whereas mouse monoclonal cytochrome c antibody (clone 7H8.2C12) was from BD PharMingen (Mississauga, ON). Rabbit anti-AIF, anti-Bax (NT) and mouse anti-FAK (clone 4.47) were purchased from upstate (Lake Placid, NY). Rabbit Akt (pan) (11E7) was obtained from Cell Signaling Technology (Beverly, MA). Mouse anti-bcl-2 oncoprotein (clone 124) was purchased at Roche (Basel, Switzerland). Anti-caspase-3 was obtained from Cell Signaling Technology (Beverly, MA). Anti-mouse Alexa 594 and 488 and anti-rabbit Alexa 488 were from Invitrogen (Burlington, ON). Horseradish peroxidase conjugated anti-mouse IgG and anti-rabbit IgG were from Amersham Canada (Oakville, Canada).

Cell Cycle Analysis by Flow Cytometry: M21, HT-29 and MDA-MB-231 cells were plated in 100-mm Petri dishes (1.5 X 10^6 cells/well) and were left to adhere at least 24 h. CEU-022 (10, 30 μM), CEU-091 (10, 30 μM), CEU-098 (10, 30 μM), CEU-236 (10 nM, 50 nM, 100 nM, 300 nM, 1 μM, 10 μM) or DMSO (0.12%) was added to the medium and incubated at 37 ˚C for 24 h. Afterwards, the adherent cells were trypsinized and pooled with the floating cells in cold PBS. The cells were next washed with PBS, and fixed in 75% ice-cold ethanol. After centrifugation, cell pellets were resuspended in PBS containing 50 μg/mL of propidium iodide and 200 μg/mL of RNase A for a total volume of 500 μL. Mixtures were incubated at room temperature for 30 min, and cell cycle distribution was analyzed with a FACScan (FACSCalibur™; Becton Dickinson, San Jose, CA).

Western Blot Analysis: The cell cycle protein levels and the presence of cleaved PARP, FAK and Akt *in situ* were evaluated by Western blotting with specific antibodies on different cell lines in two separate experiments. HT1080, MDA-MB-231 or M21 cells were seeded at 5 X 10^5 cells in 6-well plates and incubated for 16 h. Cells were treated with CEU-022 (30, 50, 100 μM), CEU-091 (30 μM), CEU-098 (30 μM), CEU-236 (1 μM), colchicine (50 nM, 50 μM), vinblastine sulfate (10 μM), or DMSO (0.12 %) for 6, 12, 18, 24, 30, 48h. After treatments, floating and adherent cells were washed in ice-cold PBS, pooled and then solubilized in SDS-PAGE buffer containing 62.5 mM Tris pH 6.8, 2 % SDS, 10 % glycerol, 0.00125 % bromophenol blue, and 15 % β-mercaptoethanol. The cell extracts were then sonicated and boiled for 5 min, separated (15μg) on 8.5 or 10 % SDS-PAGE electrophoresis gel and transferred onto a nitrocellulose membrane. All membranes were blocked and incubated with an appropriate dilution of the first antibody. Membranes were next washed and incubated with a horseradish peroxidase-conjugated goat anti-mouse or anti-rabbit IgG secondary antibody (1: 2500) (Amersham Canada, Oakville, Canada) followed by chemiluminescent detection, using an enhanced chemoluminescence (ECL) detection kit (Amersham Pharmacia Biotech).

Clonogenic Assay: The capacity of M21 human melanoma cells to form colonies was evaluated, after their treatment for 24 h, when seeded on plates pre-covered with extracellular matrices or not [1]. Treated cells were washed, trypsinized and plated at appropriate dilutions ranging from 10^2 to 10^5 M21 cells per 60-mm Petri dish. The experiments were conducted in triplicate to have approximately 50-200 viable cells per dish. Relative survival was calculated from the number of single cells that formed colonies of 50 cells within 12 days. Survival data were corrected for the plating efficiency of the appropriate controls.

Bidimensional Migration Assay: MDA-MB-231 human breast carcinoma cells were seeded at 3 X 10^5 cells in 6-well plates and incubated 7 h at 37 °C. Cells were treated with DMSO, CEU-022, CEU-091, CEU-098 or CEU-236 at 0.25, 3 or 5 μM for 16 h at 37 °C. A scratch of roughly 1000 μm was performed in the cell monolayer of each well. Floating cells were removed and, at different times (0, 3, 6, 8, 24 h), two pictures of each well were taken to evaluate the speed of the wound closure. The breach was measured three times for each picture. The migration speed of cells was determined with the slope of a graph consisting of the width of the breach as a function of time for each treatment and was the mean of two independent experiments.

Chorioallantoic Membrane (CAM) Tumor Assay: Human HT1080 fibrosarcoma and hamster CS1 melanoma cell lines were used to assess the antitumoral activity of CEU-236 in the chick chorioallantoic assay [7]. Briefly, day-0 fertilized chicken eggs were purchased from Couvoir Victoriaville (Victoriaville, Québec, Canada). The eggs were incubated for 10 days in a Pro-FI egg incubator fitted with an automatic egg turner before being transferred to a Roll-X static incubator for the rest of the incubation time (incubators were purchased from Lyon Electric, Chula Vista, San Diego, CA). The eggs were kept at 37 °C in a 60 % humidity atmosphere for the whole incubation period. Using a hobby drill (Dremel, Racine, WI), a hole was drilled on the side of the egg, and a negative pressure was applied to create a new air sac. A window was opened on this new air sac and was covered with transparent adhesive tape to prevent

contamination. A freshly prepared cell suspension (40 µL) of HT1080 (3.5 X 10^5 cells/egg) or CS1 (5 X 10^6 cells/egg) cells was applied directly on the freshly exposed CAM tissue through the window. On day 11, 100 µL of the tested drug (CEU-236, 0, 25, 50, 100 µg/mL) or the vehicle (mixture of Cremophor EL, 99% ethanol, PBS, 1:1:14 v/v) was injected in a blood vessel of the chorioallantoic membrane. Each group was composed of 12 eggs. The eggs were incubated until day-17, at which time the embryos were euthanized by putting at 4 °C followed by decapitation. Tumors were collected, pictures were taken to illustrate the different groups, and the tumor-wet weights were recorded. In all of the experiments, the number of dead embryos from the different groups was monitored for any sign of toxicity. Results are representative of three independent experiments.

Immunocytochemistry: To assess the translocation of cytochrome c, Bax or AIF, HT1080 human fibrosarcoma or M21 human melanoma cells were seeded at 1 X 10^5 cells per well in 6-well plates that contained 22-mm glass coverslips coated with fibronectin (10 µg/mL) and incubated for 24 h at 37 °C. Tumor cells were incubated either with CEU-022 (30 µM), CEU-098 (30 µM), CEU-236 (1 µM), colchicine (50 nM), vinblastine sulfate (50 nM) or DMSO (0.12 %). After 24 h treatments, the cells were washed and fixed with 3.7 % formaldehyde in PBS (pH 7.4) for 20 min. They were next permeabilized and blocked with 0.1 % saponin and 3 % (w/v) BSA in PBS. The cells were further incubated during 1 h at 37 ˚C with mouse anti-cytochrome c (clone 7H8.2C12) (1: 200) or with anti-Bax or anti-AIF polyclonal antibody (1:150) in a solution containing 0.1 % saponin and 3 % BSA in PBS. The cells were washed with PBS containing 0.05 % Tween 20™ and then incubated 1 h at 37 °C in the blocking buffer containing an anti-mouse IgG Alexa-594 (1: 1000) or an anti-rabbit IgG Alexa-488 (1:1000) with 4',6-diamidino-2-phenylindole and DAPI (2.5 µg/ml in PBS). The cellular distribution of the fluorescent cytochrome c, Bax or AIF was assessed using an Olympus BX51 microscope. Images were captured as 8-bit tagged image format files with a Q imaging RETIGA EXI digital camera driven by Image Pro Express software. Data are representative of two independent experiments.

Mitochondrial Membrane Potential ($\Delta\psi_m$) and ROS Production Analysis by FACS: HT-1080 human fibrosarcoma cells were seeded at 4 X 10^5 in a 60 mm Petri dish for 12 h. They were next incubated at 37°C with CEU-022 (30 µM), CEU-091 (30 µM), CEU-098 (30 µM), CEU-236 (2.5 µM), colchicine (100 nM) or vinblastine (5 µM) for 24, 48, 72 h or menadione (100 µM/1 h). After treatment, floating and trypsinized cells were pooled, washed and then double stained in DMEM without fetal bovine serum for 15 min at 37 ˚C with the mitochondrial membrane potential sensitive probe $DiOC_6$ (80 nM) and 5 µM dihydroethidium (HE), which acquires fluorescence upon oxidation with ROS. Treatment with the protonophore carbonyl cyanide *m*-chlorophenylhydrazone (CCCP) (100 µM/15 min) was used as negative control for $DiOC_6$ staining while menadione (100 µM/1 h), a redox cycling agent that produces ROS in the presence of O_2, was a positive control for the oxidation of HE. Fluorescence was assessed by FACScan analysis (FACSCalibur™; Becton Dickinson, San Jose, CA) in FL-1 (520 ± 20 nm) for $DiOC_6$ and FL-3 (620 ± 20 nM) for ethidium (Eth), the oxidized form of He. Dot plot analyses were performed with the WinMDI 2.8 program (J. Trotter, The Scripps Institute, La Jolla, CA) and obtained from the fluorescence data of 10000 individual cells. Cells were gated to eliminate fragments and doublets with the forward (FS) and side (SS) light scatter analysis that detects modifications of cell size and granularity, respectively. Quadrant was positioned according to the 24 h untreated dot plot to evaluate the percentage of changes in fluorescent cell distribution. The changes in optical properties of cells (size and granularity), reminiscent of cell viability loss, were determined according to the region of the 24 h untreated sample where most of cells (85%) are distributed (green), and represented on the dot plot with different colors in reference to this cell population: dark blue, diminution of size and granularity; pink, diminution of size and increase of granularity; pale blue, increase of size and granularity.

Mitochondrial Electron Microscopy Analysis: Transmission electronic microscopy was performed on MDA-MB-231 cells exposed to CEU-236 (1 µM) or DMSO (0.08 %) for 24h. Once harvested, cells were fixed 1h at 4 °C with a fixation buffer containing paraformaldehyde 2 %, glutaraldehyde 2.5 %, phosphate buffer 0.1 M pH 7.3 and calcium chloride 3 mM. Cells were washed twice with phosphate buffer 0.1 M pH 7.3 for 30 minutes then washed overnight in the same buffer. They were next fixed for a second time for 90 minutes with the same fixation buffer to which osmium tetroxide 1 % was added. The fixed cells were dehydrated with ascending alcohol concentrations, up to 100 %, followed by two propylene oxide incubations of 30 minutes. Cells were next embedded with an epoxy resin and then cured 1 day at 37 °C, followed by 3 days at 60 °C. Afterward, these samples were finely sliced (thickness of 80 nM) and placed on nickel/formvar grids (200 mesh), before being stained with lead citrate and uranil acetate. They were finally analyzed using a transmission electron microscope JEOL1230 (JEOL, Boston, Massachusetts, USA) under 80KV acceleration voltage at 6 X 10^4 and 12 X 10^4 magnification. Scale bars represent 2 µm and 100 nm for 6 X 10^4 and 12 X 10^4 magnifications, respectively.

Growth Inhibition Assay with CEM: The growth inhibition potency of CEUs, colchicine, vinblastine and taxol® was assessed using the procedure described by the National Cancer Institute for its drug screening program [19]. 96-well microtiter plates were seeded with 3.5 X 10^3 CEM and CEM-VLB cells suspended in 100 µL of RPMI supplemented with 10% fetal bovine serum. Drugs freshly solubilized in DMSO were diluted in culture medium and aliquots of 100 µL containing sequential dilution of drugs were added. Final drug concentrations ranged from 100 to 1 µM for CEU-022, -091, -098, from 100 to 0.01 µM for CEU-236, from 100 µM to 0.1 nM for colchicine and from 1 µM to 0.01 nM for vinblastine. Plates were incubated for 48 h. The incubation was stopped by addition of cold trichloroacetic acid to the wells (10 % final concentration), followed by incubation for 1 h at 4 °C. Plates were washed five times with water. Sulforhodamine B solution (50 µL) at 0.1 % (w/v) in 1 % acetic acid was added to each well, and plates were incubated for 15 min at room temperature. After staining, unbound dye was removed by washing five times with 1 % acetic acid. Bonded dye was solubilized with 10 mM Tris base, and the absorbance was read using a µQuant Universal Microplate Spectrophotometer (Biotek, Winooski, VT) at 585 nm. Background optical density from a control reference plate fixed on the day of treatment was subtracted from the O.D obtained with the 48-h growth period. The growth inhibition percentage was calculated in reference to DMSO treated cells for each drug concentrations. The results were obtained from at least 3 separate experiments. The GI_{50} assay was considered valid when the variability among data for a given set of conditions, within the same experiment, was less than 10 % with respect to the mean value.

Extracellular Matrices (ECMs): Native (Col IV) and heat-denatured type IV collagen (HdCol IV) (50 µg/ml), fibronectin (FN) (25 µg/ml), fibrinogen (Fg) and fibrin (Fb) (50 µg/ml) were used to coat non-adherent tissue culture plates (Nunc). After washes with serum-free DMEM, M21 cells were plated in serum-containing or serum-free media on the different matrices and incubated overnight. Moreover, 5 X 10^5 cells were plated in 6-well plates for Western blot analysis of FAK, Akt and PARP and 1 X 10^6 cells were plated in 100-mm Petri dishes coated with different ECMs. Forthwith, M21 cells were challenged with CEU-022 (100 µM), colchicine (50 µM) and vinblastine (10 µM) for Western blot analysis or CEU-022 (20 µM) for clonogenic assay. Representative data resulting from two independent experiments performed in triplicate are shown.

Plasmid, Transfection and Cell Viability Assay: The pEGFP-C3-hBcl-2 (EGFP-Bcl-2) construct was kindly provided by Dr. Richard J. Youle. HT1080 cells were seeded at 1 X 10^6 cells per 60 mm dish and incubated 12 h at 37 °C. They were next transfected with 0.5 µg/mL of each plasmid and 4 µL of the FuGENE 6 reagent per µg of pcDNA3 or pEGFP-C3-hBcl-2, according to the manufacturer's instructions (Roche Diagnostics, Indianapolis, IN). Twenty-four hours post-transfection, cells (3500/well) were seeded in 96-well plates and incubated at 37 °C for 5 h. Fresh medium containing DMSO, CEU-022 (20 µM), CEU-091 (20 µM), CEU-098 (20 µM), CEU-236 (1 µM), colchicine (15 µM) or vinblastine (10 nM) was added, and cells were further incubated at 37 °C for 24 h. Resazurin (25 µg/mL) was next

added to the culture medium for 1 h at 37 °C. Cell viability was calculated from fluorescence (excitation, 530 nm; emission, 590 nm) measured with a FL 600 Reader (Bio-Tek Instruments, Winooski, VT). Data from experiments conducted in triplicate were corrected for the background fluorescence of the medium and were expressed as the mean percentage of fluorescence obtained for control DMSO-treated cells. They are representative of two independent experiments.

RESULTS

Mitotic Arrest and CDK1/cyclin B Expression Level Induced by CEUs: We first evaluated and compared the antimitotic potency of CEUs by assessing their effect on the cell cycle using three different types of cancer cell lines (MDA-MB-231, M21 and HT-29). Cells were treated with different concentrations of each drug. CEU-022 and CEU-098 are bioisosteric derivatives while CEU-091 is the non-alkylating counterpart of CEU-022.

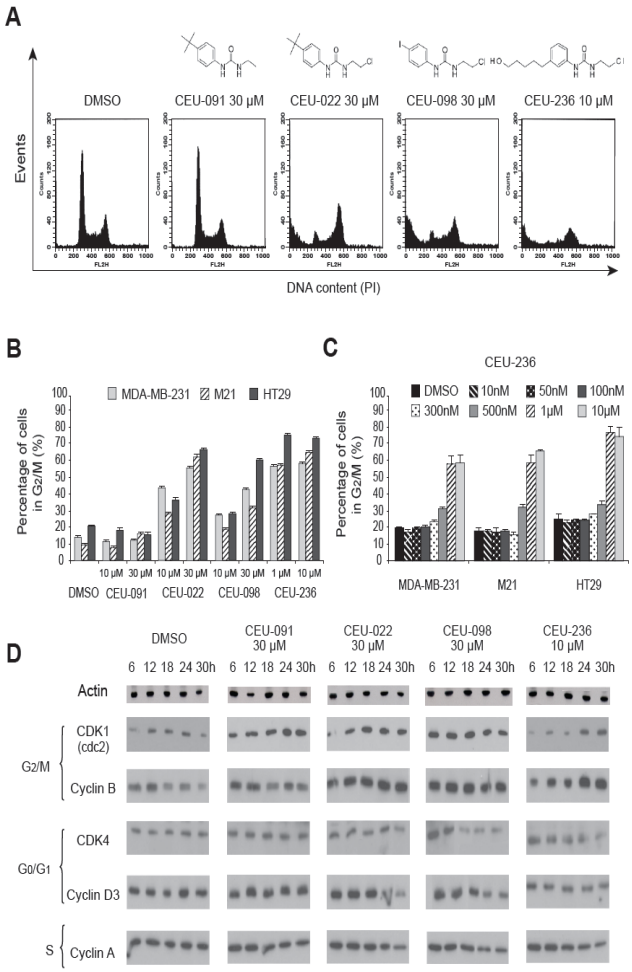

Fig. 1: Mitotic arrest (A, B, C) and increased of CDK1/cyclin B expression level (D) in response to CEUs.

CEU-236 exhibits a bulky and polar substituent at the position 3 of the aromatic moiety (Figure 1A). As was previously shown for antimicrotubule agents such as *vinca* alkaloids and taxanes, β-tubulin alkylating CEU-022 and CEU-098, CEU-236 also blocks cell division at the G_2/M phase (Figure 1A and B). However, CEU-91 did not seem to have any effect on the cell cycle at 10 µM and 30 µM CEU-091. MDA-MB-231, M21 and HT-29 cell accumulation in G_2/M phase were observed at 10 µM and were predominant at 30 µM for CEU-022 and CEU-098 (Figure 1B). CEU-236 exhibited strong accumulation in G_2/M phase at concentrations lower than its counterparts (1 and 10 µM). Dose-dependent analysis of CEU-236, illustrated in Figure 1C, demonstrates that the G_2/M block occurred at 500 nM and is maximal when using 1 µM for the three cancer cell types. Afterwards, we analyzed kinetic protein levels of different cyclins and CDKs on MDA-MB-231cells treated with CEUs (Figure 1D). In comparison to the control DMSO, antimitotic CEUs, notably compounds CEU-022 and -236, induced an increase in the cyclin B/CDK1 protein levels and a decrease in the cyclin D3/CDK4 protein levels; these changes generally started 12 to 24 hours after treatment. Antimitotic CEUs did not induce significant changes in cyclin A (Figure 1D) or in CDK2 and cyclin E protein levels (data not shown).

CEUs are Potent Cytotoxic and Antiangiogenic Agents: Several CEUs were previously shown to not only inhibit cancer cell proliferation, but also abrogate endothelial cell migration [1, 3]. We therefore completed dose-dependent studies to compare CEU effects on cell growth and migration (Figure 2). Clonogenic assays showed that CEU-022 and CEU-098 exhibit a strong inhibition on cancer cell growth at 30 µM and CEU-236 at 5 µM. While CEU-091 seemed to have little impact, CEU-236 had the highest cell growth inhibition potency on M21 cells as compared to other CEUs, colchicine and vinblastine (Figure 2A). The bidimensional assay performed using the highly mobile MDA-MB-231 cells showed that CEU-236 displayed a strong motogenic inhibition on the evaluated tumor cells (Figure 2B). While CEU-022 and CEU-098 diminished MBA-MB-231 migration at 5 µM, a subcytotoxic concentration, CEU-236 had similar effects at much lower concentrations (0.5 µM) and impeded both cell growth and migration at 5 µM. Of note, CEU-091, which is devoid of alkylating moiety, neither impeded M21 cell growth nor MBA-MB-231 cell migration.

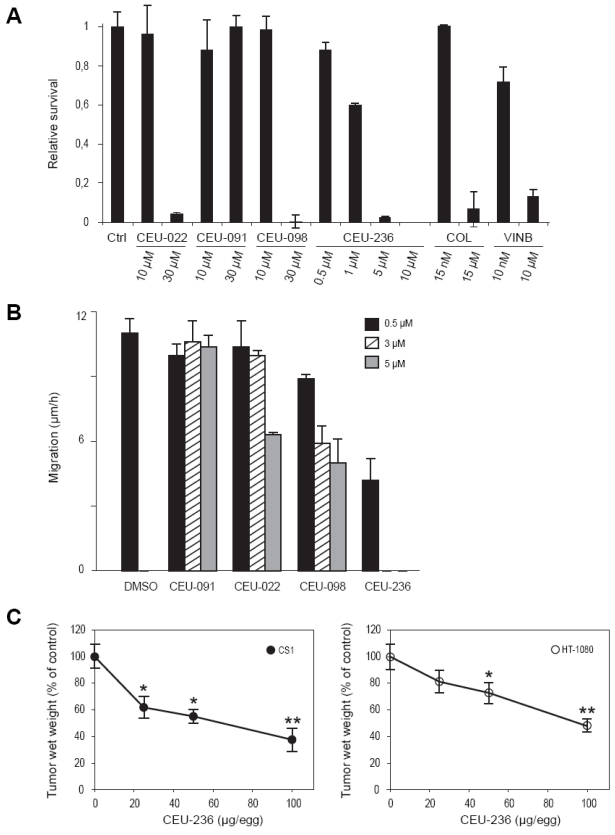

Fig. 2: Antimitotic CEUs display anti-proliferative (A), anti-migration (B) and anti-tumoral (C) properties.

ANOVA test showed a significant difference between doses ($P < 0.01$). Dunnett test was performed (*, $P < 0.05$; and **, $P < 0.01$).

The strong anti-proliferative and anti-motogenic potency of CEU-236 prompted us to evaluate the growth of solid tumors in the chick CAM model (Figure 2C). The growth of solid tumors on the surface of the CAM depends on its ability to stimulate angiogenesis and to grow significantly in 7 days. CS1 hamster melanoma and HT1080 human

fibrosarcoma cell lines were used for their potency to produce solid tumors sensitive to antiangiogenic and antitumoral therapy [1]. Incubation of CS1- and HT1080-derived tumors on the CAM with CEU-236 reduced significantly the tumors size in a dose-dependent manner (Figure 2C), as previously published for CEU-022 and -098 [1]. Both CS1- and HT1080-derived tumor masses were inhibited by CEU-236 in the same concentration range. Interestingly, the tumor masses were devoid of grossly visible blood vessels as compared to the vehicle (data not shown). The concentrations of CEU-236 used appeared to be well tolerated by the chick embryos since no mortality was observed.

CEUs Promote Bax Translocation to Mitochondria: Antimitotic CEUs, like other commonly used antimicrotubule drugs, have been shown to reduce cellular adhesion and provoke disorganization of focal adhesion and actin stress fibers that precedes the onset of anoikis [5]. We demonstrated that sustained phosphorylation of paxillin required the activation of p38 [5].

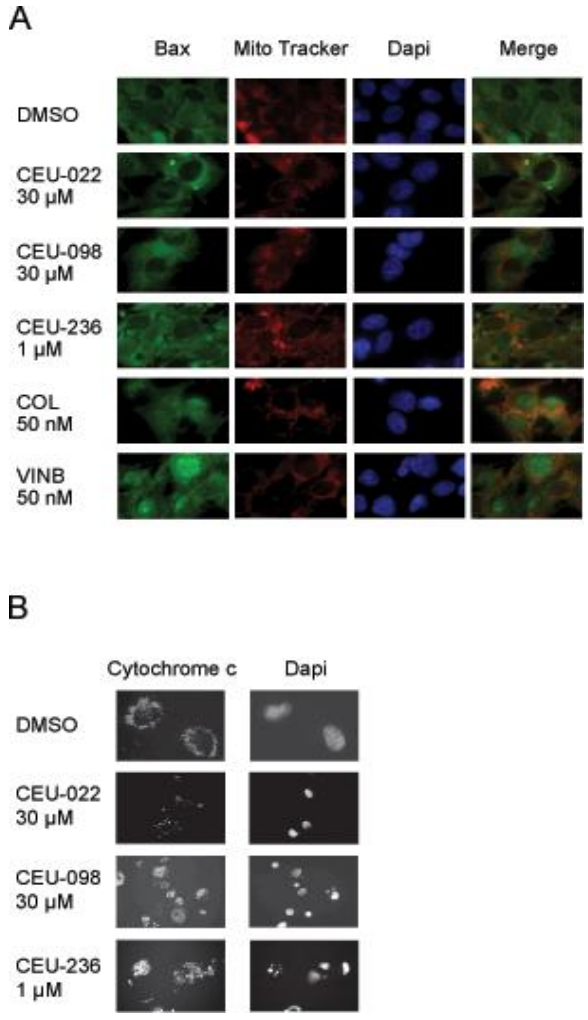

Fig. 3: CEUs induce Bax mitochondrial translocation (A), cytochrome c release (B), nuclear condensation and fragmentation (B).

Herein, we studied the mitochondrial sequence of events leading to anoikis with our compounds. Bax, a member of the Bcl-2 protein family, plays a key role in the mitochondrial potential lost, the formation of transition pores and the release of apoptotic protein mediators such as cytochrome c and AIF in response to different stimuli, such as the increase of reactive oxygen species (ROS), thiol oxidation and loss of the mitochondrial membrane potential ($\Delta\psi_m$) [20]. Phosphorylation of Bim is required to induce the translocation of Bax into the mitochondria [11, 13]. We analyzed the localisation of Bax following 24 h treatments of M21 melanoma cells (Figure 3A). Bax translocation into the mitochondria of M21 cells occured in response to CEU-022, CEU-098 and CEU-236. Colchicine and vinblastine induced the translocation of Bax into the nucleus. This translocation occurred to a lesser extent in cells treated with DMSO.

CEUs Induce the Onset of the Classical Apoptosis Pathway: Cytochrome c Mitochondrial Release, Nuclear Condensation and Fragmentation: We have shown previously [1] and herein that CEUs inhibit cell proliferation and are cytotoxic, as demonstrated in clonogenic assay. We investigated whether the common effectors of cell death, such as cytochrome c mitochondrial release, mediated the cytotoxic activity of CEUs. In a first set of experiments, we showed that cytochrome c localization was critically modified following CEU-022, -098 and -236 treatments in HT1080 (Figure 3B). The release of cytochrome c from mitochondria was also observed with MDA-MB-231 cells (data not shown). Furthermore, nuclear condensation and fragmentation occurred following exposure to any of the antimitotic CEUs used in the present study (Figure 3B).

CEU-Treated Cells Exhibit Loss of Mitochondrial Membrane Potential, ROS Production and Mitochondrial Morphological Alterations: ROS production and loss of membrane potential ($\Delta\psi_m$) are two manifestations that occur during the early phase of apoptosis [20]. We monitored the $\Delta\psi_m$ and the ROS production changes in HT1080 cells with the cationic $DiOC_6$ and dihydroethidium (HE) probes, respectively. Treatment with the protonophore carbonyl cyanide m-chlorophenylhydrazone (CCCP) (100 µM/15 min) was used as negative control for $DiOC_6$ staining. Menadione (100 µM/1 h), a redox cycling agent that produces ROS in the presence of O_2, was selected as a positive control for the oxidation of HE. Anti-mitotic CEUs (except CEU-091) led to a drop in $\Delta\psi_m$ and an increase in ROS production (Figure 4A); changes were similar in the other anti-microtubule agents tested (vinblastine and colchicine). ROS production was observed 24 h following antimitotic CEUs, and was markedly with CEU-236, colchicine and vinblastine conditions. The loss of $\Delta\psi_m$ started 24 h after CEUs colchicine and vinblastine treatments and increased greatly after a treatment of 48 and 72 h. CEU-236 exhibited a pattern similar to that of colchicine and provoked a marked reduction of the cell size. The reduction of cell size and granularity was indicative of an increase in cell mortality at 48 and 72 h following CEUs, colchicine and vinblastine treatment. We then observed the appearance of mitochondria in MDA-MB-231 cells using electronic microscopy to investigate the capacity of CEU-236 to initiate apoptosis. MDA-MB-231 cells treated with DMSO for 24 h showed ultrastructural details representative of normal cells, with no or negligible changes seen in the mitochondria (Figure 4B). Progressive damage to MDA-MB-231 cells treated with CEU-236 (1 µM) was obvious after 24 h, and multiple mitochondria showed marked swelling as well as typical large matrix compartments (Figure 4B).

In some cells, this process progressed to a final stage, with extensive vacuolization and nuclear pyknosis. The characteristic condensation and peripheral margination of nuclear chromatin, hallmarks of apoptosis, were observed following CEU-236 treatment.

CEUs Provoke PARP Cleavage and AIF Nuclear Translocation. Cleavage-dependent activation of the initiator caspase-9 and caspase-8 are hallmarks for the initiation of apoptosis. Previous studies showed the activation of caspase-9, -6, -7, -3, -8, and PARP cleavage following CEU-022, CEU-098 and CEU-236 treatments [3, 5]. To determine the contribution of caspase activation on PARP cleavage in response to antimitotic CEU treatments, HT1080 cells were pretreated for 1 h with the caspase inhibitor N-benzyloxycarbonyl-Val-Ala-Asp-fluoromethylketone (zVAD.fmk) (Figure 5A and B). Pretreatment with zVAD.fmk decreased the cleavage of PARP for CEU-022, CEU-236 and colchicine (Figure 5B). Those observations were noticed in a lesser extend with CEU-098. For the colchicine conditions the PARP protein level expression increased with the decrease in cleaved protein following zVAD.fmk pretreatment as compared to the non-pretreated cells.

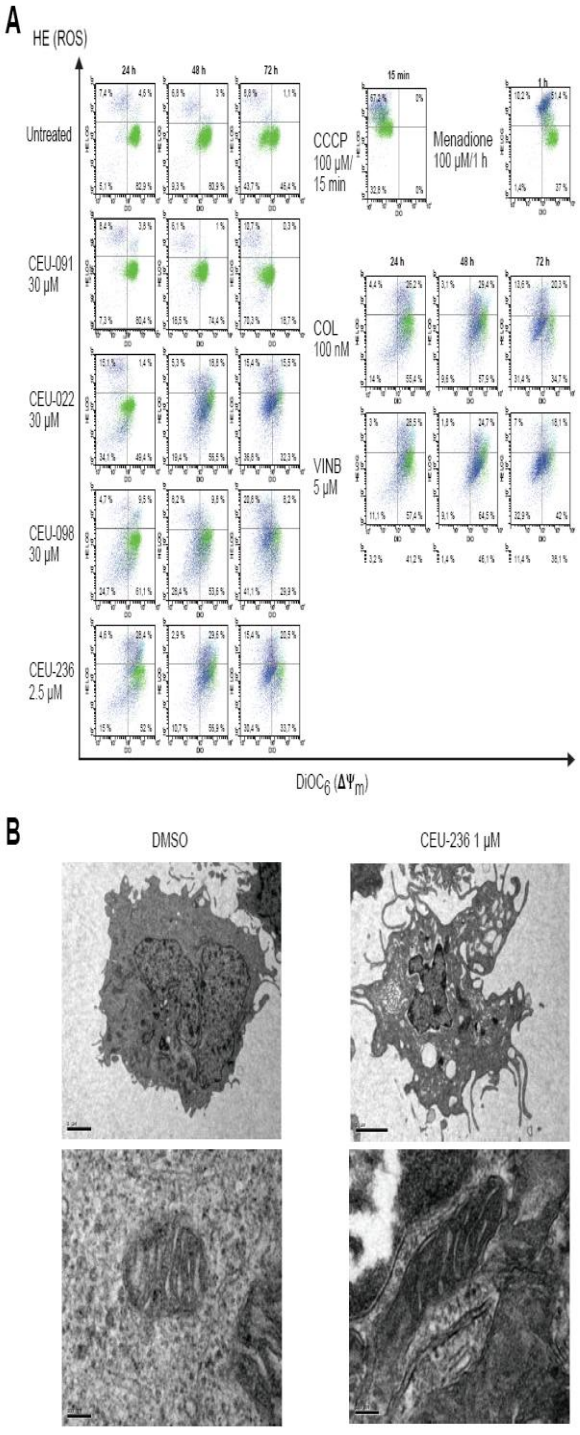

Fig. 4: Loss of mitochondrial membrane potential ($\Delta\psi_m$) and ROS production induced by CEUs using (A) FACScan and (B) transmission electronic microscopy analysis of mitochondria.

The proper use of the caspase inhibitor is shown in Figure 5A, which demonstrates the reduction in caspase-3 cleavage in zVAD.fmk pretreated cells. Since nuclear condensation was observed following CEU treatment (Figure 3C) and knowing that AIF triggers nuclear condensation, we further evaluated whether the intracellular localization of AIF in M21 changed after the exposition to antimitotic CEUs. Immunocytochemistry showed that CEUs induced AIF nuclear translocation in a fashion similar to colchicine, but less than vinblastine (Figure 5C).

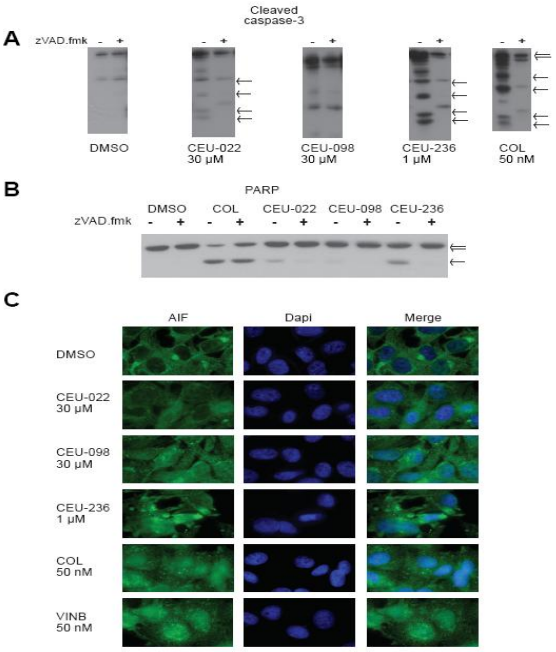

Fig. 5: CEUs induce the proteolytic cleavage of proteins associated with apoptosis (caspase-3 (A), PARP (B)) and AIF nuclear translocation (C). Double and single arrows indicate the native and cleaved protein respectively.

P-glycoprotein, ECMs, or Bcl-2 Overexpression do not Protect Cells From CEUs: Previous studies demonstrated that CEU-022 exhibits equivalent anti-proliderative activity in cells with either P-glycoprotein overexpression, increased intracellular concentration of gluthatione and/or glutathione-S-transferase activity, altered topoisomerase II activity or increased DNA repair mechanisms. The multidrug resistance phenotype (MDR1) mediated by P-glycoprotein (Pgp) is an important mechanism of resistance to the microtubule-targeting drugs such as *vinca* alkaloids and taxanes, as well as a broad range of other classes of anticancer agents [4]. We therefore used cells overexpressing P-glycoprotein (CEM-VLB) or not (CEM) and treated them with common antimitotics and CEUs (Figure 6). CEU-098, CEU-236 remained potent antiproliferative agents even in CEM-VLB cells, as opposed to colchicine, vinblastine.

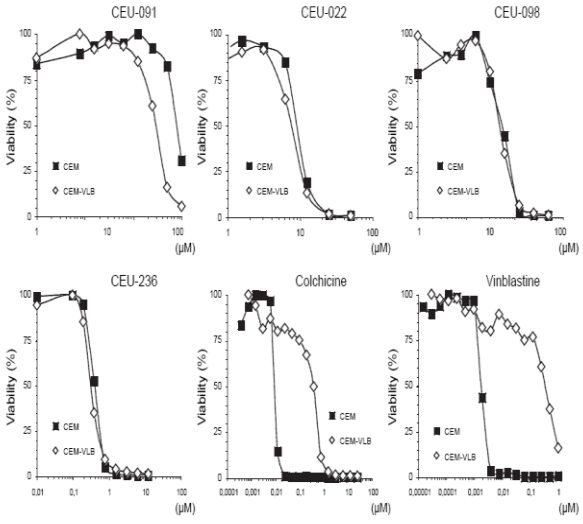

Fig. 6: CEUs display cytotoxic activity on cells exhibiting P-glycoprotein overexpression (MDR1).

The tumor microenvironment can modulate the ability of tumor cells to overcome antineoplastic treatment, such as cisplatin, and involves integrins to trigger prosurvival signals [18]. The CAM-DR phenotype is caused by integrin/extracellular matrix (ECM)-induced pro-survival signal. We evaluated the potency of CEU-022, as a representative of other potent CEUs, colchicine and vinblastine to trigger FAK, Akt and PARP cleavage in M21 cells seeded on different extracellular matrices (ECMs): native (Col IV) and heat-denatured type IV collagen (Hd), fibronectin (FN), fibrinogen (Fg) and fibrin (Fb) (Figure 7A). ECMs reduce PARP cleavage for colchicine- and vinblastine-treated cells. FAK and Akt cleavage were totally inhibited by the presence of ECMs after colchicine and vinblastine exposure. Interestingly, CEU-022 induced FAK, Akt and PARP cleavage under all conditions tested (Figure 7A) and abrogated significantly the survival of M21 cells seeded with ECMs fibrin, fibrinogen and native collagen compared to the condition without FBS and matrix (Figure 7B).

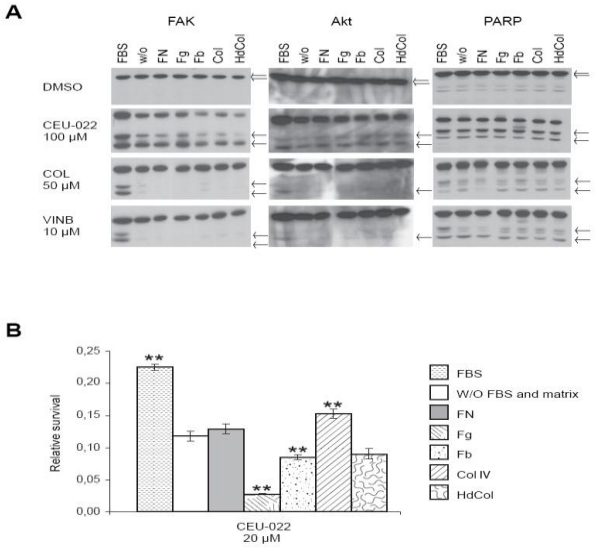

Fig. 7: ECM does not protect cells from CEU-022 damage, such as FAK, Akt and PARP cleavage (A) and cell death (B).

Dunnett test was performed (** $P < 0.01$) for comparison with the condition without FBS and matrix.

The Bcl-2 oncoprotein can inhibit apoptosis induced by antitumor agents at a point downstream of drug-target interactions [9]. The ability of Bcl-2 to enhance cell viability (Figure 8) was studied with PEGFP-Bcl-2 transfected HT1080 cells. As depicted in Figure 8, Bcl-2 protein overexpression significantly increased cell viability following exposure to colchicine for 24 h, but not following exposure to CEU-022, CEU-098 or CEU-236. CEUs maintained their anti-proliferative activity in both transfected cell populations ($pcDNA_3$ and pEGFP-Bcl-2).

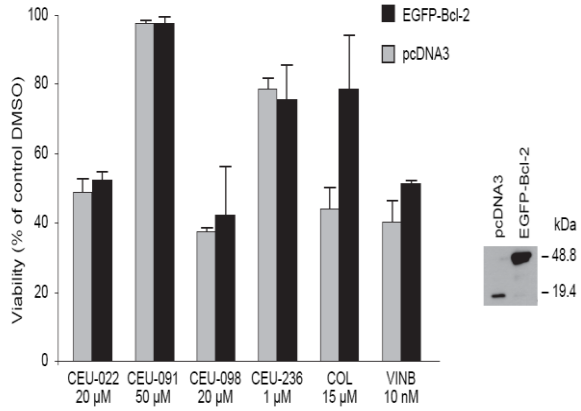

Fig. 8: CEUs are unaffected by Bcl-2 overexpression.

DISCUSSION

Our results showed that the major signaling route underlying the anti-proliferative action of CEUs is similar to the other well-known anti-microtubule agents, including colchicine and vinblastine [8]. As opposed to these classical agents, CEUs bind covalently and irreversibly to β-tubulin through an acylation reaction [2]. While paclitaxel stabilizes microtubule dynamics, colchicine and vinblastine destabilize microtubules and prevent further addition or loss of subunits [8]. Colchicine forms a tubulin-drug complex, which then copolymerizes into the microtubule ends, thus suppressing the microtubule dynamics even when their ends remain competent to grow. On the other hand, CEUs bind the soluble-β-tubulin pool and inhibit microtubule growth.

As with other commonly used antimicrotubule agents, CEU-022, CEU-098 and CEU-236 provoke a G_2/M cell cycle arrest. Herein, we showed a dose-dependent increase in the percentage of cells accumulated in the G_2/M cell cycle phase. Antimicrotubule drugs block the proteasome-dependent degradation of cyclin B1, resulting in a sustained activation of cyclin B1/cdc2 kinase and a cell cycle arrest in mitosis. Likewise, these agents induce also an up-regulation of cyclin B1 and CDK1/cdc2 proteins and stimulate their activity. The CDK1/cyclin B protein levels raised in accordance with the blockage observed in G_2/M. However, the population of cells in the G_0/G_1 phase diminished, with a progressive accumulation of cells arrested in G_2/M phase (data not shown), consequently the CDK4/cyclin D3 protein level was reduced (Figure 1).

Except for CEU-236, CEUs are cytotoxic at doses higher than other common anti-mitotic agents (Figure 2A). However, they induce mitotic arrest (Figure 1A, 1B) in the same concentration ranges as their anti-proliferative activity (Figure 2A). This is not the case for other common antimicrotubule agents, including colchicine and vinblastine, which are not cytotoxic at anti-proliferative doses (nM range) [21, 22]. Accordingly, efficient repolymerization of microtubules has been shown to restore normal cell cycle and growth during the long lag phase observed between microtubule disruption by those drugs and the onset of apoptosis [8]. This highlights the importance of timing in signaling and duration to achieve a final outcome with these drugs [8]. Noteworthy, due to irreversible and covalent binding to β-tubulin, cells exposed to anti-proliferative doses of alkylating CEUs cannot be rescued [5].

Some microtubule-disrupting agents act on tumor vasculature and inhibit angiogenesis. At low-dose and non-cytotoxic concentrations, proliferation, adhesion and migration of human endothelial cells have been shown reduced by potent antimicrotubule agents such as colchicine, *vinca* alkaloids and taxotere [21, 22]. Compared to normal and cancer cells, vascular endothelial cells were preferentially affected by continuous low-dose exposure to the drugs that exhibit antiangiogenic properties in several *in vitro* models [21, 22]. Clinical application of a continuous low dose of these agents has thus been suggested as an optimal way of delivering antiangiogenic cancer therapy [22]. The efficacy of classical microtubule-targeted agents as either antiproliferative agents or as vascular-targeting agents might reside in their pharmacokinetic and pharmacodynamics characteristics, the reversibility of their binding to tubulin and their lack of long-term retention in cells. Agents that enter cells, depolymerize microtubules and are metabolized or excreted rapidly might act best as antivascular agents. Those that are retained in cells and induce long-term mitotic block might work best as antiproliferative agents that induce apoptotic cell death, such as CEU-022 and CEU-098. Interestingly, CEU-236 exhibited both anti-motogenic and cytotoxic potency in the micromolar range (Figure 2A, 2B). We evaluated the antiangiogenic and antitumor potency of CEU-236 in the chick embryo CAM assay. CEU-236 diminished significantly the tumor size, as observed previously with CEU-022 and CEU-098 [1]. Tumors were also devoid of obvious blood vessels (data not shown), also supporting that antimitotic CEUs have both potent antiendothelial and antitumor cell activity *in vivo* [1].

The focal adhesion disassembly in response to CEUs, in addition to the mitotic spindle disruption, may contribute significantly to reach

the cellular threshold for the onset of apoptosis through anoikis [5, 8, 9]. We therefore investigated the mechanisms underlying the adhesion impairment and the cytotoxic properties of CEUs. Antimitotic CEUs trigger apoptosis involving, in part, the release of cytochrome c from the permeability transition pore complex (PTPC) in the external membrane of the mitochondria. Cytochrome c plays an essential role in apoptosis, as shown in cell lines from mice that have a disrupted gene and are refractory to apoptosis induced by stimuli that affect mitochondria [14]. However, cytochrome c release alone does not appear to be sufficient to trigger apoptosis [14].

Following classical anti-mitotic treatment, it has been described that Bim, inducing the oligomerization of BAK and Bax, leads to cytochrome c release [14]. The CEUs tested herein provoked Bax translocation into the mitochondria, leading to subsequent cytochrome c release. The translocation of Bax is accompanied by apparent changes in Bax conformation, unmasking its N-terminus and resulting in Bax oligomerization, which promotes the permeabilization of the outer mitochondrial membrane [14]. Released intermembrane space proteins included cytochrome c, which complexes with Apaf-1 (apoptotic protease-activating factor 1) and caspase-9 to form a post-mitochondrial apoptosome that amplifies effector caspase activation [14]. M21 cells treated with colchicine or vinblastine also induced Bax translocation into the mitochondria, as did CEUs. Cells treated with colchicine or vinblastine also have high levels of Bax protein levels in their nucleus (Figure 3B). Translocation of Bax into the nucleus during apoptosis has previously been reported after exposure of cells to hyperthermia. Bax may play an important role both within the nucleus in the early phase of apoptosis as well as in the mitochondrial membrane.

Variations in mitochondrial membrane potential ($\Delta\psi_m$) are key events during drug-induced apoptosis [20]. Herein, we described that CEU-236, the most potent of the anti-mitotic CEUs tested, induced ROS production, loss of $\Delta\psi_m$, and mitochondrial swelling. We demonstrated the translocation of the mitochondrial protein AIF (apoptosis-inducing factor), a caspase-independent death effector, into the nucleus of CEU-treated M21 cells. Nuclear condensation and fragmentation were observed after CEU treatment. Furthermore, a previous study demonstrated that the initiator caspase-9 is cleaved rapidly after CEU or colchicine treatment (as early as 6 hours for CEU-098 and CEU-236), and the effector caspases (-3, -6 and -7) followed in the next hours [5]. Such a sequence of activation is coherent with a caspase-mediated cell death. Pro-survival proteins such as FAK, Akt and PARP were cleaved following anti-mitotic and CEU treatments [3, 5]. Thus, for those compounds, mitochondria play a key role in the control of cell death execution [14]. Altogether, these observations indicate that CEUs induce apoptosis in cancer cells.

We then treated with our compounds a variety of cancer cells, which normally exhibit mechanisms of resistance towards anticancer treatment. Drug resistance is a major factor hampering the clinical anti-cancer efficacy of microtubule targeting agents. The multidrug resistance phenotype mediated by P-glycoprotein (Pgp) is an important mechanism of resistance to the microtubule-targeting drugs *vinca* alkaloids and taxanes, as well as a broad range of other classes of anti-cancer agents [8]. These drugs are excluded from cells expressing p-glycoprotein and its overexpression results in resistance to these compounds. This probably constitutes the most efficient mechanism for cancer cells to achieve resistance to many structurally and mechanistically unrelated drugs, a phenomenon known as multidrug-resistance (MDR) [6]. Herein, we demonstrated that antimitotic CEUs preserve their growth inhibition properties in the presence of Pgp overexpression (Figure 6).

Previous studies report that the cytotoxicity of cisplatin could be reduced by ECMs such as collagens, fibronectin and laminins, which are integrin ligands. There is an increased recognition that different ECMs abrogate the efficacy of anticancer drugs. This mechanism is named the CAM-DR phenotype and is caused by integrin/extracellular matrix (ECM)-induced pro-survival signals. We demonstrated that the cytotoxicity of CEU-022 (used as a representative member of this class) was unaffected by fibrin and fibrinogen matrix, as opposed to cisplatin [1]. Herein, we demonstrate that apoptotic signaling events, such as FAK, Akt and PARP cleavage, remain strongly present in cells seeded on ECM and treated with CEU-022, in contrast to colchicine and vinblastine treatment. Moreover, CEU-022 provoked the death of M21 cells seeded or not on the different ECMs. Cells that overexpress the pro-survival proteins Bcl-2 and Bcl-XL are highly resistant to anoikis [17]. Interestingly, anti-mitotic CEUs preserve their antiproliferatic activity in cells transfected with pEGFP-Bcl-2. On the other hand, there was a significant inverse correlation between growth inhibition by colchicine and Bcl-2 levels. Bcl-2 serves as a powerful antidote to cell death and may countermand the effect of both caspase-dependent and independent modes of cell death through manifold-independent functions such as the abrogation of cytochrome c release from mitochondria, the regulation of calcium homeostasis, the promotion of glutathione sequestration to the nucleus, and the modulation of antioxidant pathways.

In conclusion, we identified unique properties of antimitotic CEUs, which are β-tubulin acylating agents and promising antineoplastics. We have shown previously that antimitotic CEUs display a sustained inhibition of the β-tubulin polymerization and a parallel dismantlement of focal adhesion [5, 24]. Herein, we demonstrated that these events lead to the production of ROS and loss of mitochondrial membrane potential. The mitochondrial translocation of Bax following CEU treatments, which is known to be involved in the formation of a permeability transition pore [11-13, 23]. These events are followed by classical apoptotic features such as the release of mitochondrial cytochrome c and AIF, caspase activation, pro-survival protein cleavage, and nuclear condensation and fragmentation (Figure 9) [9]. Antimitotic CEUs preserve their anti-proliferative activity against MDR resistance phenotype, CAM-DR pro-survival signal, and Bcl-2 overexpression. Moreover, we demonstrated that CEU-236 is a potent anti-proliferative and anti-motogenic agent in the micromolar range. CEU-236 is active in the chick embryo CAM and is 20-fold more potent than most of the previously prepared CEUs. This compound is of utmost interest since the presence of oxygenated group(s) significantly alters the physicochemical properties of the drugs and probably results in a different biodistribution profile from that of CEU-022 and CEU-098. The pharmacomodulation of CEU-236 therefore opens a new area of research and medical application.

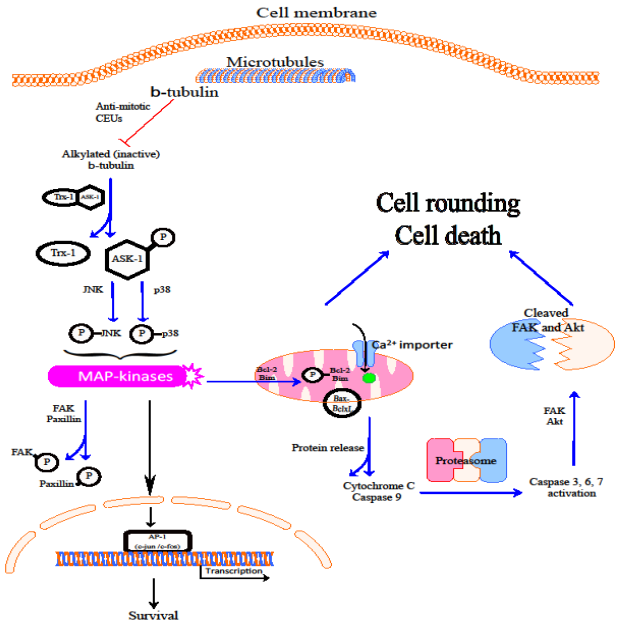

Fig. 9: Proposed biochemical pathway for anti-mitotic CEUs induced apoptosis.

Anti-mitotic CEUs alkylate β-tubulin and induce a stress on the cytoskeleton inducing changes such as actin contraction. The dissociation of ASK-1 and thioredoxin-1 (Trx-1) complex occurs in

cells treated with anti-mitotic CEUs [24]. Ask-1 is subsequently phosphorylated and triggers the phosphorylation of JNK and P38. Consequently, paxillin phosphorylation by the MAPKs leads to focal adhesion disorganization. In addition, the antiapoptotic protein Bcl-2 and the pro-apoptotic BH3-only protein Bim are phosphorylated and mitochondrial translocation of Bax occurs. Cytochrome c, procaspase-9 and Apaf-1 are released from mitochondria and form a complex leading to caspase activation. Prosurvival proteins such as FAK and Akt are cleaved through the activated caspases. These events lead to apoptosis and anoikis.

ABBREVIATIONS LIST

AIF, apoptosis-inducing factor; Apaf-1, apoptotic protease-activating factor-1; ASK-1, apoptosis signal regulating kinase-1; BSA, bovine serum albumin; CAM, chick chorioallantoic membrane assay; CAM-DR, cell adhesion mediated drug resistance; cDDP, cisplatin, cis-platinum(II)diammine dichloride; CEU, *N*-aryl-*N'*-(2-chloroethyl)ureas; CEU-022, 4-*tert*-butyl-chloroethylurea; CEU-025, 4-cyclohexyl-chloroethylurea; CEU-098, 4-iodo-chloroethylurea; COL, colchicine; Vb, vinblastine; ECM, extracellular matrix; ERK, extracellular signal-regulated kinase; FA, focal adhesion; FAK, focal adhesion kinase; IEG, immediate early gene; JNK, c-jun NH_2-terminal kinase; L-JNKI-1, L-stereoisomer of a peptide inhibitor of c-jun NH_2-terminal Kinase; MAP, mitogen-activated protein; MDR, multiple drug resistance; MIA, microtubule interfering agents; MT, microtubule; MAPK, mitogen-activated protein kinase; PD098059, 2-(2-amino-3-methoxy-phenyl)chromen-4-one; PTCPC, permeability-transition pore complex; SB203580, 4-(4-fluorophenyl)-2-(4-methylsulfinylphenyl)-5-(4-pyridyl)-1*H*-imidazole; PX-12, 1-methylpropyl 2-imidazolyl disulfide; Trx, thioredoxin isoform 1.

ACKNOWLEDGEMENT

This work was supported by grants from the Canadian Institute for Health Research (R.C-G; grant #MOP-79334 and #MOP-89707). Jessica S. Fortin was recipient of a studentship from the Fonds de la Recherche en Santé du Québec. We are very grateful to Mrs. Josée Boulet for the conception of some of the illustrations and Mr. Maurice Dufour for the FACS analyses and technical advice.

REFERENCES

1. Petitclerc E, Deschesnes RG, Cote MF, Marquis C, Janvier R, Lacroix J, et al. Antiangiogenic and antitumoral activity of phenyl-3-(2-chloroethyl)ureas: a class of soft alkylating agents disrupting microtubules that are unaffected by cell adhesion-mediated drug resistance. **Cancer Res** 2004; 64 (13):4654-63.
2. Bouchon B, Papon J, Communal Y, Madelmont JC, Degoul F. Alkylation of prohibitin by cyclohexylphenyl-chloroethyl urea on an aspartyl residue is associated with cell cycle G(1) arrest in B16 cells. **Br J Pharmacol** 2007; 152 (4):449-55.
3. Patenaude A, Deschesnes RG, Rousseau JL, Petitclerc E, Lacroix J, Cote MF, et al. New soft alkylating agents with enhanced cytotoxicity against cancer cells resistant to chemotherapeutics and hypoxia. **Cancer Res** 2007; 67 (5):2306-16.
4. Wiesen KM, Xia S, Yang CP, Horwitz SB. Wild-type class I beta-tubulin sensitizes Taxol-resistant breast adenocarcinoma cells harboring a beta-tubulin mutation. **Cancer Lett** 2007; 257 (2):227-35.
5. Deschesnes RG, Patenaude A, Rousseau JL, Fortin JS, Ricard C, Cote MF, et al. Microtubule-destabilizing agents induce focal adhesion structure disorganization and anoikis in cancer cells. **J Pharmacol Exp Ther** 2007; 320 (2):853-64.
6. Zhou J, Giannakakou P. Targeting microtubules for cancer chemotherapy. **Curr Med Chem Anticancer Agents** 2005; 5 (1):65-71.
7. Rixe O, Fojo T. Is cell death a critical end point for anticancer therapies or is cytostasis sufficient? **Clinical Cancer Research** 2007; 13 (24):7280-7.
8. Mollinedo F, Gajate C. Microtubules, microtubule-interfering agents and apoptosis. **Apoptosis** 2003; 8 (5):413-50.
9. Okada H, Mak TW. Pathways of apoptotic and non-apoptotic death in tumour cells. **Nature Reviews Cancer** 2004; 4 (8):592-603.
10. Wang XH, Cheung HW, Chun ACS, Jin DY, Wong YC. Mitotic checkpoint defects in human cancers and their implications to chemotherapy. **Frontiers in Bioscience-Landmark** 2008; 13:2103-14.
11. Lei K, Davis RJ. JNK phosphorylation of Bim-related members of the Bcl2 family induces Bax-dependent apoptosis. **Proc Natl Acad Sci USA** 2003; 100 (5):2432-7.
12. Papadakis ES, Finegan KG, Wang X, Robinson AC, Guo C, Kayahara M, et al. The regulation of Bax by c-Jun N-terminal protein kinase (JNK) is a prerequisite to the mitochondrial-induced apoptotic pathway. **Febs Letters** 2006; 580 (5):1320-6.
13. Marani M, Tenev T, Hancock D, Downward J, Lemoine NR. Identification of novel isoforms of the BH3 domain protein Bim which directly activate Bax to trigger apoptosis. **Molecular and Cellular Biology** 2002; 22 (11):3577-89.
14. Birbes H, Luberto C, Hsu YT, Bawab SEL, Hannun YA, Obeid LM. A mitochondrial pool of sphingomyelin is involved in TNF alpha-induced Bax translocation to mitochondria. **Biochemical Journal** 2005; 386 :445-51.
15. Jahani-Asl A, Basak A, Tsang BK. Caspase-3-mediated cleavage of Akt: Involvement of non-consensus sites and influence of phosphorylation. **Febs Letters** 2007; 581 (16):2883-8.
16. Flusberg DA, Numaguchi Y, Ingber DE. Cooperative control of Akt phosphorylation, bcl-2 expression, and apoptosis by cytoskeletal microfilaments and microtubules in capillary endothelial cells. **Molecular Biology of the Cell** 2001; 12 (10):3087-94.
17. Reginato MJ, Mills KR, Paulus JK, Lynch DK, Sgroi DC, Debnath J, et al. Integrins and EGFR coordinately regulate the pro-apoptotic protein Bim to prevent anoikis. **Nature Cell Biology** 2003; 5 (8):733-40.
18. Gilmore AP, Metcalfe AD, Romer LH, Streuli CH. Integrin-mediated survival signals regulate the apoptotic function of Bax through its conformation and subcellular localization. **Journal of Cell Biology** 2000; 149 (2):431-46.
19. Shoemaker RH. The NCI60 human tumour cell line anticancer drug screen. **Nature Reviews Cancer** 2006; 6 (10):813-23.
20. Fleury C, Mignotte B, Vayssiere JL. Mitochondrial reactive oxygen species in cell death signaling. **Biochimie** 2002; 84 (2-3):131-41.
21. Hayot C, Farinelle S, De Decker R, Decaestecker C, Darro F, Kiss R, et al. In vitro pharmacological characterizations of the anti-angiogenic and anti-tumor cell migration properties mediated by microtubule-affecting drugs, with special emphasis on the organization of the actin cytoskeleton. **International Journal of Oncology** 2002; 21 (2):417-25.
22. Bocci G, Nicolaou KC, Kerbel RS. Protracted low-dose effects on human endothelial cell proliferation and survival in vitro reveal a selective antiangiogenic window for various chemotherapeutic drugs. **Cancer Res** 2002; 62 (23):6938-43.
23. Letai A, Bassik MC, Walensky LD, Sorcinelli MD, Weiler S, Korsmeyer SJ. Distinct BH3 domains either sensitize or activate mitochondrial apoptosis, serving as prototype cancer therapeutics. **Cancer Cell** 2002; 2 (3):183-92.
24. Fortin J, Patenaude A, Deschesnes RG, Cote MF, Petitclerc E, R CG. ASK1-P38 pathway is important for anoikis induced by microtubule-targeting aryl chloroethylureas. **J Pharm Pharm Sci** 2010; 13 (2):175-90.